Melting of small Arctic ice caps observed from ERS scatterometer time series

Laurence C. Smith,[1,2] Yongwei Sheng,[1] Richard R. Forster,[3] Konrad Steffen,[4] Karen E. Frey,[1] and Douglas E. Alsdorf[1]

Received 29 April 2003; revised 20 June 2003; accepted 5 August 2003; published 21 October 2003.

[1] Time series of active microwave backscatter data from the ERS Wind Scatterometers are used to demonstrate (1) the timing of melt onset can be observed over small ice caps, as well as the major ice sheets and multi-year sea ice; and (2) temporally integrated backscatter reduction (R) is strongly correlated with total annual positive-degree-days (PDD), as measured at four automated weather stations on the surface of the Greenland Ice Sheet. The latter is particularly interesting because unlike melt onset, R is a measure of melt processes integrated over an entire ablation season. Both methods work owing to the well-known sharp decrease in radar backscatter triggered by the appearance of liquid water in a glacier snowpack. Melt onset and R are determined for 14 small Arctic ice caps from 1992–2000. Interannual and regional variability in the timing of melt onset are comparable, averaging 33 ± 9 and 38 ± 13 days, respectively. Regional variability in R exceeds interannual variability, averaging 906 ± 164 and 309 ± 130 dB·d, respectively. The brevity of the derived nine-year records limits their statistical testing for trend. However, their qualitative interpretation suggests that the timing of melt onset is more variable for Arctic ice caps than for sea ice, and the intensity of summer surface melting increased by about 20% in the 1990s. *INDEX TERMS:* 1827 Hydrology: Glaciology (1863); 3349 Meteorology and Atmospheric Dynamics: Polar meteorology; 1863 Hydrology: Snow and ice (1827); 1640 Global Change: Remote sensing; 6969 Radio Science: Remote sensing. **Citation:** Smith, L. C., Y. Sheng, R. R. Forster, K. Steffen, K. E. Frey, and D. E. Alsdorf, Melting of small Arctic ice caps observed from ERS scatterometer time series, *Geophys. Res. Lett.*, *30*(20), 2034, doi:10.1029/2003GL017641, 2003.

1. Introduction

[2] Excluding the Greenland ice sheet, the Arctic contains about 40% of the world's small glaciers and ice caps. Field measurements of glacier mass-balance suggest that most have been losing volume in recent decades, contributing an estimated 0.13 mm/yr to global sea-level rise [*Dowdeswell*, 1995; *Dowdeswell et al.*, 1997]. As such, they supply roughly half of the contribution to mean sea level rise estimated for small glaciers globally [~25 mm/yr, *Dyurgerov and Meier*, 1997]. However, a known problem with such estimates is that they are based on a small group of field-accessible glaciers, with associated size and distribution biases. Observed trends are also difficult to interpret climatically, owing to a near-nonexistence of meteorological data from glacier accumulation zones. For most glaciers, the duration and intensity of summer melting drive ablation losses, the primary negative term in the glacier mass balance. Satellite remote sensing therefore has considerable appeal as a tool for detecting melt processes on remote glacier surfaces.

[3] Spaceborne Ku- and C-band radar scatterometers have been successfully used to detect the timing of melt onset over the major ice sheets of Antarctica and Greenland [*Long and Drinkwater*, 1999; *Drinkwater and Liu*, 2000; *Wismann*, 2000; *Nghiem et al.*, 2001]. The method works because the appearance of liquid water in snow dramatically increases microwave absorption and decreases penetration depth and volume scattering [*Ulaby et al.*, 1981]. The resulting sharp backscatter decrease is coincident or nearly so with the rise of local air temperatures above 0°C, and is now a well-known phenomenon associated with melt onset over glaciers and sea ice [e.g., *Rott and Matzler*, 1987; *Winebrenner et al.*, 1994; *Smith et al.*, 1997; *Yueh and Kwok*, 1998; *Forster et al.*, 2001]. Here, we show that total annual melting intensity can also be determined, by temporally integrating the backscatter reduction (R) over the entire ablation season. Using ERS scatterometer data, both melt onset and R are derived for fourteen Arctic ice caps from 1992–2000, and the observed variability and possible trends discussed.

2. Timing and Intensity of Surface Melting From ERS Scatterometer Time Series

[4] Wind Scatterometer data were obtained by the ERS-1 satellite from 1991–1996, with measurements since March 1996 obtained by ERS-2. Problems with the ERS-2 spacecraft attitude and orbital control made data unavailable beginning January 2001. Both instruments recorded C-VV radar backscattering coefficients (σ^0) at 45, 90, and 135° beams to the right of the spacecraft flight direction. All available daily raw backscatter σ^0 were corrected to values predicted for an incident angle of 40° (σ^0_{40}) and processed to a 25 km polar stereographic grid according to *Sheng et al.* [2002]. Near-daily time series of σ^0_{40} were generated for single-cell targets centered over fourteen study Arctic ice caps and automated weather stations (AWS) in Greenland (Table 1, Figure 1). Approximate target elevations were determined from ETOPO5 5-minute elevation data. Ice cap

[1]Department of Geography, University of California, Los Angeles, USA.
[2]Department of Earth & Space Sciences, University of California, Los Angeles, USA.
[3]Department of Geography, University of Utah, Salt Lake City, USA.
[4]Cooperative Institute for Research in Environmental Sciences (CIRES), University of Colorado, Boulder, USA.

0094-8276/03/2003GL017641$05.00

Table 1. Physical and 1992–2000 Melt Characteristics of Ice Cap Targets on Figure 1

Site #	Name	Lat.	Long.	elev. (m)	area (km^2)	$\bar{M}$	M_{min}	M_{max}	$\bar{R}$	R_{min}	R_{max}
1	Muller (Axel Heiberg Island)	79.90	−90.98	1372	994	190[a]	179	204	245[a]	145	356
2	Devon Island (Devon Island)	75.33	−83.19	1281		185[a]	154	205	337[a]	169	600
3	Cadogan (Ellesmere Island)	78.22	−77.06	914	798	173[a]	153	192	536[a]	405	677
4	Agassiz (Ellesmere Island)	80.40	−75.00	1493		189[a]	173	207	181	100	271
5	Barnes (Baffin Island)	70.25	−74.20	899		164[a,b]	152	181	187[a,b]	171	237
6	Auyuittuo (Baffin Island)	67.40	−66.54	1791		174[b]	153	184	473[b]	335	709
7	Hans Tausen (Greenland)	82.50	−38.33	975		179[a]	169	198	307	59	475
8	Negibreen (Svalbard)	78.67	18.67	305	1180	175	165	191	647[b]	568	778
9	Austfonna SE (Svalbard)	79.58	25.00	366	2230	178	167	195	1049	916	1390
10	Moskvy (Franz Josef Land)	80.35	57.85	91	504	178	166	195	482	383	584
11	Vetrenyy (Franz Josef Land)	80.78	63.53	152	728	179	170	193	540	354	642
12	Novaya Zemlya N (Novaya Zemlya)	75.90	64.00	366		175	156	188	760	639	1006
13	Academy of Sciences (Severnaya Zemlya)	80.55	94.82	671	4540	192	173	216	541	292	815
14	Vavilov Ice Cap (Severnaya Zemlya)	79.32	96.00	305	1806	183	168	216	348	166	485

$\bar{M}$ = Average Melt Onset (Day-of-Year), M_{min} = Earliest Onset, M_{max} = Latest Onset, $\bar{R}$ = Average R (dB·d), R_{min} = Minimum R, R_{max} = Maximum R Over Period of Record.
[a]1992 missing.
[b]1993 missing.

area, where available, was obtained from the World Glacier Inventory [*NSIDC*, 1999].

2.1. Melt Onset

[5] To automate extraction of melt-onset date from σ^0_{40} time series, the detection algorithms of *Joshi et al.* [2001] and *Forster et al.* [2001] were modified as follows. After convolution with a derivative-of-Gaussian filter, onset was determined as the first day when (1) a specified threshold in backscatter drop was exceeded; and (2) the contrast between eight-day means of σ^0_{40} immediately preceding and following the drop also exceeded a specified threshold. Step (2) further eliminates from consideration possible ''false starts'' in melt onset. A dynamic threshold of $k(r)^{1/2}$ was used in both steps, where r is the difference between mean winter and median summer backscatter at each site and k a user-defined constant. Through trial and error, an optimal value of 1.1 was identified for k. The required threshold for melt onset was not exceeded at sites 4, 7 in 1992, precluding extraction of melt onset. Low data density also precluded computation of melt onset at sites 1, 2, 3, 5, in 1992 and sites 5, 6 in 1993.

2.2. Melt Intensity

[6] For each site, a measure of annual melt intensity was estimated using the metric of ''temporally integrated σ^0_{40} reduction'' proposed by *Wismann* [2000]. The metric presumes that prolonged and/or intense melt seasons are manifested as prolonged and/or greater reductions in radar backscatter over the same time interval, and is computed as:

$$R = \sum_{i=1}^{n} \left(\overline{\sigma^0_{40\,w}} - \sigma^0_{40\,i} \right) \quad (1)$$

where the temporally integrated σ^0_{40} reduction (R) represents the summation from June 1 (i = 1) to September 30 (i = n) of the contrast between daily values of σ^0_{40} and the respective mean winter backscatter for the preceding period November 1–March 31 ($\overline{\sigma^0_{40\,w}}$). Annual time series of R were constructed from 1992 to 2000 for each of the fourteen Arctic ice caps in Table 1. Low data density precluded computation of R at sites 1, 2, 3, 5 in 1992 and sites 5, 6, 8 in 1993.

[7] Using NCAR/NCEP surface air temperature reanalysis data, *Wismann* [2000] shows a linear correlation between R and ''temporally integrated positive air temperatures,'' or positive degree-days (PDD). In this paper, the validity of R as a measure of melt intensity is tested using real AWS meteorological data of the Greenland Climate Network (GC-NET) [*Steffen and Box*, 2001]. Time series of σ^0_{40} were generated for single 25 km grid cells corresponding with each of eighteen GC-NET AWS. Melt signatures were detected at six stations. Two were discarded owing to proximity to another station and suspect data quality, respectively. Hourly air temperature measurements collected 2 m above the glacier surface were used to compute total summer PDD at the remaining four AWS at Crawford Point (1995–2000), DYE-2 (1996–2000), Saddle (1997–2000) and S-Dome (1997–2000) (Figure 1).

3. Observations

[8] All σ^0_{40} time series from ice cap interiors show melt onset signatures similar to large ice sheets and multi-year sea-ice environments (Figure 2). Robust signatures from sites in the Russian Arctic, where melt onset on surrounding first-year sea ice is otherwise difficult to detect [*Yueh and Kwok*, 1998; *Forster et al.*, 2001], provide further confidence that they are glacier-derived. Table 1 shows means, maxima and minima of melt onset day-of-year for the period 1992–2000. Melt onset anomalies for individual years show considerable scatter (Figure 3), with little

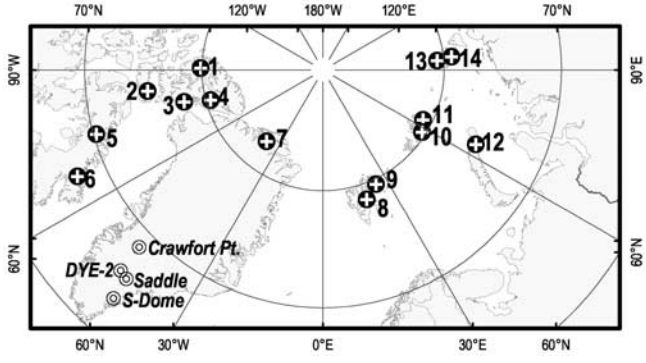

Figure 1. Locations of study ice caps and four GC-NET automated weather stations, used for validation of R.

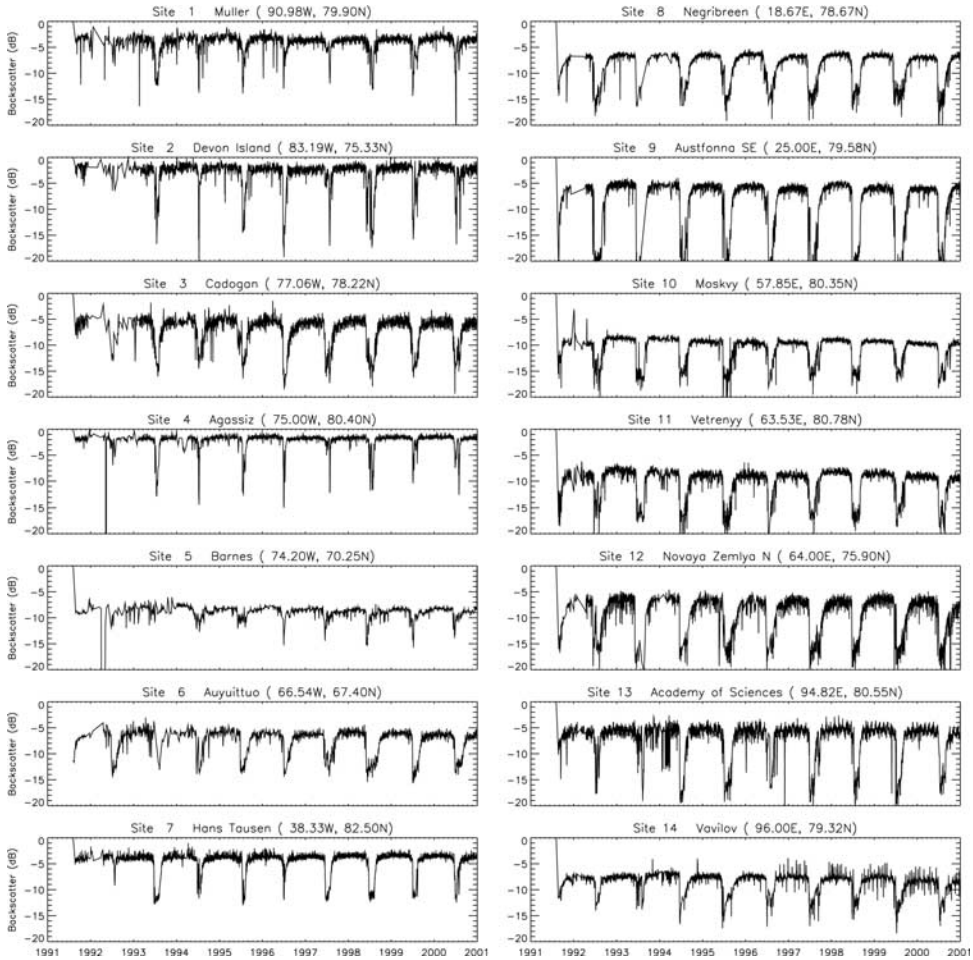

Figure 2. Time series of corrected radar backscatter σ^0_{40} for single-cell targets listed in Table 1. Sharp reductions in backscatter reduction are caused by ice surface melting. Temporally integrated backscatter reduction (R) summates the magnitude of this reduction from June 1 to September 30 of each year.

suggestion of trend. Strong regional and interannual variability is found, likely owing to spring frontal activity [*Forster et al.*, 2001]. Interannual variability ($M_{max} - M_{min}$) ranges from 23 (Vetrenyy) to 51 days (Devon Island), with an average value of 33 ± 9. This is comparable to the interannual variability of melt onset over Arctic sea ice, which averages three weeks or less [*Anderson*, 1987; *Smith*, 1998] to a month or more [*Robinson et al.*, 1992]. Regional variability ranges from 22 (1994) to 60 days (1993), with an average value of 38 ± 13. This exceeds the regional variability of melt onset over sea ice, which typically takes only 2–3 weeks to progress from the marginal seas to the pole [*Smith*, 1998; *Rigor et al.*, 2000]. A plausible reason for this contrast is that ice cap elevations vary nearly 2000 m between sites (Table 1).

[9] A strong positive linear correlation (r^2 = 0.89) is found between satellite-derived values of R and AWS-derived PDD data (Figure 4). This result is interesting because unlike melt onset, R is a measure of melt processes

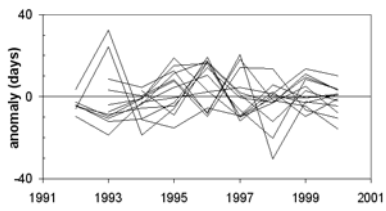

Figure 3. Melt onset anomalies for all ice caps, 1992–2000.

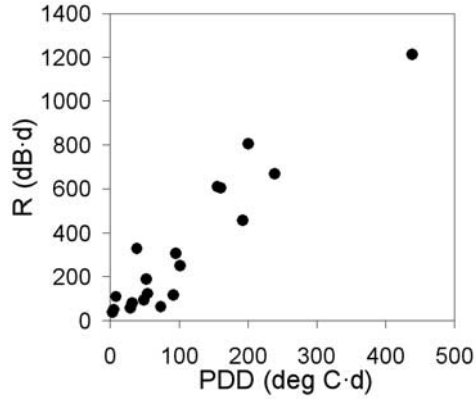

Figure 4. Empirical relationship between R and total summer positive degree-days (PDD), at four GC-NET AWS. Linear regression yields $R = 2.84(PDD) + 22.2$ ($r^2 = 0.89$).

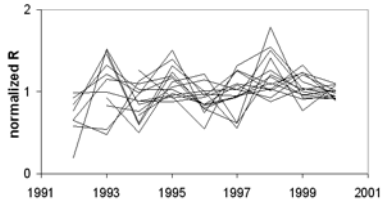

Figure 5. Normalized *R* time series for all ice caps, 1992–2000. Melt intensity increases approximately twenty percent over the period of record.

integrated over the entire ablation season. A likely explanation for this correlation is that longer periods of above-zero air temperatures both prolong the duration of suppressed radar backscatter and also increase PDD. Regardless of physical mechanism, the co-variance of *R* and PDD seen at four AWS sites suggests that *R* time series may be used as a relative, and perhaps quantitative, indicator of melt intensity over ice caps. It is tempting to apply the linear relationship between *R* and PDD (Figure 4) to transform all *R* time series to PDD. However, more AWS data are required to ascertain if the correlation remains linear for the larger values of PDD typical of warmer, lower-elevation sites. It is plausible that a threshold in backscatter reduction may be attained, whereby further increases in PDD do not yield further increases in *R*. If so, *R* may be more a function of the number of above-zero days (PD) rather than positive degree-days (PDD). However, our results suggest that scatterometer data may be used to empirically estimate PDD for high-elevation or high-latitude glaciers where total summer PDD does not exceed 500. Elsewhere, *R* may be applied as a proxy for melt duration and/or intensity.

[10] Not surprisingly, mean values of *R* generally decrease with ice cap elevation and latitude (Table 1). Interannual variability ($R_{max} - R_{min}$) varies from 66 (Barnes) to 523 dB·d (Academy of Sciences), with an average value of 309 ± 130. Regional contrasts vary from 742 (1995) to 1250 dB·d (1999), with an average value of 906 ± 164. Absolute values of *R* vary up to one order of magnitude between test sites, likely owing to latitudinal, elevation and possibly ice facies differences. Interannual variations in melt intensity generally fluctuate within ±20% of their long term means (Figure 5) except on Severnaya Zemlya, where melt intensity can vary more than 100%. Although brevity of the time series in Figure 5 prevents statistically significant testing for trend, their qualitative assessment suggests a general increase in ice cap melting of about 20% for the decade.

4. Concluding Remarks

[11] Melt onset has attracted considerable attention in scatterometer studies of the cryosphere, in part because it yields a robust radar signature easily seen across different platforms and ice surface types. However, the date of melt onset alone is of limited value for remotely assessing the total intensity or duration of glacier melting over a full annual cycle. Also uncertain is whether interannual variations in melt onset are diagnostic of secular climatic patterns and trends, or instead reflect short-term stochastic variability of frontal systems. Temporally integrated backscatter reduction (*R*) is a time-integrated measure of the prevalence and/or duration of surface melting, and is therefore a more encompassing measure of interannual variations in glacier ablation losses. These losses appear to have increased over small Arctic ice caps from 1992 to 2000, but the record is short. Further investigation will be enabled by continued deployment of satellite wind scatterometers, such as the ESA Advanced Scatterometer (ASCAT) planned for launch in 2005.

[12] **Acknowledgments.** This project was funded by NASA. ERS scatterometer data were acquired by the European Space Agency and provided by IFREMER CERSAT, Plouzané, France.

References

Anderson, M. R., The onset of spring melt in first-year ice regions of the Arctic as determined from scanning multichannel microwave radiometer data for 1979 and 1980, *J. Geophys. Res.*, *92*(C12), 13,153–13,163, 1987.

Dowdeswell, J. A., Glaciers in the high Arctic and recent environmental change, *Phil. Trans. Royal Soc. London Ser. A*, *352*(1699), 321–334, 1995.

Dowdeswell, J. A., et al., The mass balance of circum-Arctic glaciers and recent climate change, *Quat. Res.*, *48*(1), 1–14, 1997.

Drinkwater, M. R., and X. Liu, Seasonal to interannual variability in Antarctic sea-ice surface melt, *IEEE Trans. Geosci. Remote Sens.*, *38*(4), 1827–1842, 2000.

Dyurgerov, M. B., and M. F. Meier, Year-to-year fluctuations of global mass balance of small glaciers and their contribution to sea-level changes, *Arctic Alpine Res.*, *29*(4), 392–402, 1997.

Forster, R. R., et al., The onset of Arctic sea-ice snowmelt as detected with passive- and active-microwave remote sensing, *Ann. Glaciol.*, *33*, 85–93, 2001.

Joshi, M., et al., An edge detection technique to estimate melt duration, season and melt extent on the Greenland ice sheet using passive microwave data, *Geophys. Res. Lett.*, *28*(18), 3497–3500, 2001.

Long, D. G., and M. R. Drinkwater, Cryosphere applications of NSCAT data, *IEEE Trans. Geosci. Remote Sens.*, *37*(3), 1671–1984, 1999.

National Snow and Ice Data Center, *World Glacier Inventory* (digital media), Boulder, CO, 1999 (updated 2003).

Nghiem, S. V., et al., Detection of snowmelt regions on the Greenland ice sheet using diurnal backscatter change, *J. Glaciol.*, *47*(159), 539–547, 2001.

Rigor, I. G., et al., Variations in surface air temperature observations in the Arctic, 1979–97, *J. Climate*, *13*, 896–914, 2000.

Robinson, D. A., et al., Large-scale patterns and variability of snowmelt and parameterized surface albedo in the Arctic Basin, *J. Climate*, *5*(10), 1109–1119, 1992.

Rott, H., and C. Matzler, Possibilities and limits of synthetic aperture radar for snow and glacier surveying, *Ann. Glaciol.*, *95*, 195–199, 1987.

Sheng, Y., et al., A high temporal-resolution dataset of ERS scatterometer radar backscatter for research in Arctic and sub-Arctic regions, *Polar Record*, *38*(205), 121–126, 2002.

Smith, D. M., Observation of perennial Arctic sea ice melt and freeze-up using passive microwave data, *J. Geophys. Res.*, *103*(C12), 27,753–27,769, 1998.

Smith, L. C., et al., Seasonal climatic forcings on alpine glaciers revealed with orbital synthetic aperture radar, *J. Glaciol.*, *43*, 480–488, 1997.

Steffen, K., and J. E. Box, Surface climatology of the Greenland ice sheet: Greenland climate network 1995–1999, *J. Geophys. Res.*, *106*(D24), 33,951–33,964, 2001.

Ulaby, F. T., et al., Microwave remote sensing: Fundamentals and radiometry, Volume I., Artech House, Norwood, MA, 456 pp., 1981.

Winebrenner, D. P., et al., Observation of melt onset on multiyear Arctic sea ice using the ERS 1 synthetic aperture radar, *J. Geophys. Res.*, *99*(C11), 22,425–22,441, 1994.

Wismann, V., Monitoring of seasonal snowmelt on Greenland with ERS scatterometer data, *IEEE Trans. Geosci. Remote Sens.*, *38*(4), 1821–1826, 2000.

Yueh, S. H., and R. Kwok, Arctic sea ice extent and melt onset from NSCAT observations, *Geophys. Res. Lett.*, *25*(23), 4369–4372, 1998.

L. C. Smith, Y. Sheng, K. E. Frey, and D. E. Alsdorf, Department of Geography, University of California, Los Angeles, USA. (lsmith@geog.ucla.edu)

R. R. Forster, Department of Geography, University of Utah, Salt Lake City, USA.

K. Steffen, Cooperative Institute for Research in Environmental Sciences (CIRES), University of Colorado, Boulder, USA.